NEUROTOXICIY OF VANADIUM EXPOSURE: COMPARATIVE REGIONAL PREVALENCE OF NEUROPATHOLOGIES

J. Olopade[1], I.A. Azeez[1], C. Laperchia[2], A. Andrioli[2], M. Bentivoglio[2]

- Abstract Number: FENS-0770 – Poster Board Number: C137

Address: [1]Department of Veterinary Anatomy, University of Ibadan, Nigeria, [2]Department of Movement and Neurological sciences, University of Verona, Italy.

Email: **James O. Olopade***- jkayodeolopade@yahoo.com; Idris A. Azeez- eedreez505@gmail.com; Claudia Laperchia- cla.laperchia@gmail.com; Anna Andrioli-anna.andrioli@gmail.com; Marina Bentivoglio- marina.bentivoglio@univr.it

INTRODUCTION

Environmental exposure to vanadium has been on the increase particularly in areas of persistent burning of fossil fuels. Vanadium exposure is known to induce oxidative stress, and the assessment of the histopathological correlates of neurotoxicity of this metal remains an area of ongoing research. We here characterized myelin, glial cell response and cytokine expression in a murine model of vanadium toxicity.

MATERIALS AND METHODS

Young adult BALB/c mice were used for this study. The dams were administered 3mg/kg b/w NaVO3 ip from postnatal day (P)1 through 21. Pups were then dosed 3 times a week from P22 to P89. Matched controls were administered vehicle. On P90, mice were sacrificed and the brains processed for the histochemical visualization of myelin (using Black Gold staining), and immunophenotyping of astrocytes, microglia, as well as expression of the pro-inflammatory cytokines tumor necrosis factor (TNF)-alpha and interleukin (IL)-1beta. Single and multiple labeling was used, in bright-field and confocal microscopy.

RESULTS AND DISCUSSION

Chronic vanadium administration resulted in marked loss of myelinated axons in the cerebral cortex and subcortical white matter, corpus callosum, internal capsule. Astrocyte and microglia activation was widespread, with regional prevalence in the telencephalon and diencephalon. Striking induction of TNF-alpha expression was found, especially in the hippocampus, where the cytokine was found to be expressed in astrocytes. IL-1beta induction prevailed instead in diencephalic regions.

CONCLUSION

The present findings point to widespread vanadium-induced brain damage, represented by demyelination and a marked neuroinflammatory response, with a regional prevalence that could account for diverse functional effects.

REFERENCES

Aschner M, Edward DL., Cristina S, Olopade JO, Kirsten JH, Daiana SA, Damiyon S, Rahim HA, Upchurch L, Donerly S, Elwood L., Anna F, Padmavathi P, and Connor JR (2010) : **Gene-Environment Interactions: Neurodegeneration in Non-Mammals and Mammals.** *Neurotoxicology*, 31(5):582–588.

Garcia GB, Biancardi ME. Quiroga AD (2005) : **Vanadium (V)-Induced Neurotoxicity in The Rat Central Nervous System: A Histo-Immunohistochemical Study.** *Drug and Chemical Toxicology*, 28(3):329-344.

Igado OO, Olopade JO, Onwuka SK, Chukwudi AC, Daramola OA, Ajufo UE (2008) : **Evidence of environmental pollution in caprine brains obtained from a relatively unindustrialized area in Nigeria.** *African Journal of Biochemical Research* , 11:305–309.

ACKNOWLEDGEMENT

The authors are grateful to the ISN-CAEN for the financial aid for this work.

FIGURES

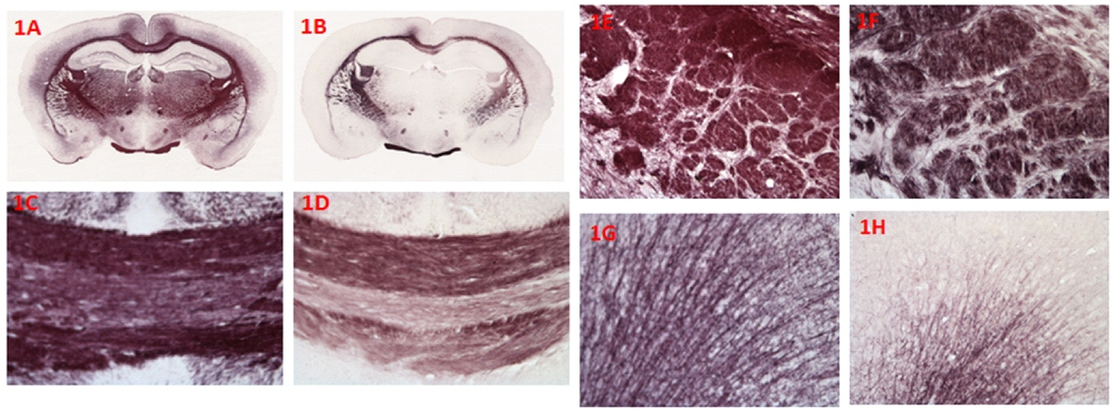

Figure 1: Myelin histoarchitecture following vanadium exposure.
Mosaic views (Figs. **1A** and **1B**) of black gold stained brain sections reveal depleted axons traversing the cortices and pale large myelin tracts, Mg .x40. High power views, x100 of corpus callosum (**1C**. and **1D**.), Internal capsule (**1E** and **1F**) and the motor cortex (**1G** and **1H**) shows paleness and depletion of myelin and shortened axons in the cortex.

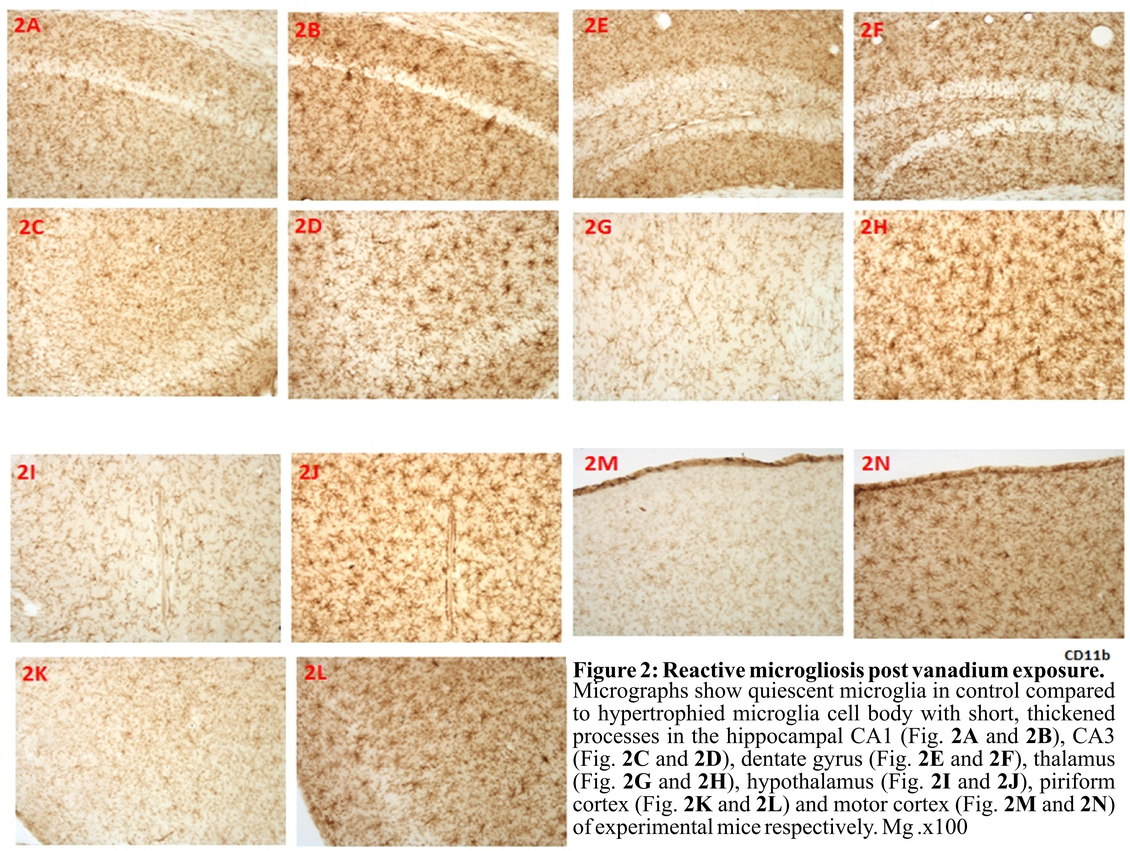

Figure 2: Reactive microgliosis post vanadium exposure.
Micrographs show quiescent microglia in control compared to hypertrophied microglia cell body with short, thickened processes in the hippocampal CA1 (Fig. **2A** and **2B**), CA3 (Fig. **2C** and **2D**), dentate gyrus (Fig. **2E** and **2F**), thalamus (Fig. **2G** and **2H**), hypothalamus (Fig. **2I** and **2J**), piriform cortex (Fig. **2K** and **2L**) and motor cortex (Fig. **2M** and **2N**) of experimental mice respectively. Mg .x100

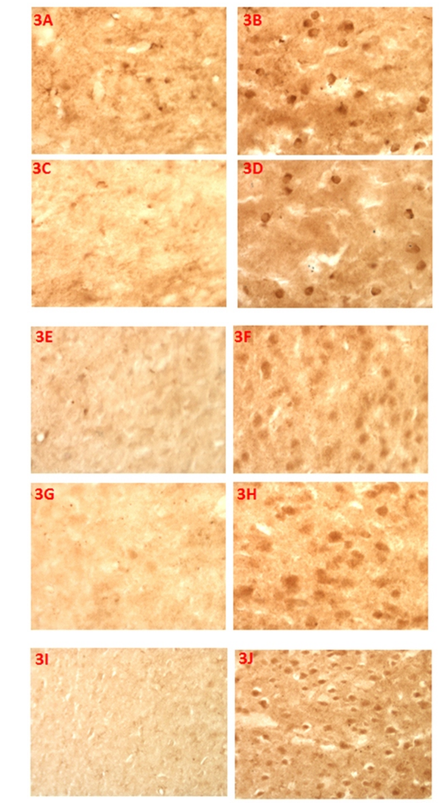

Figure 3:

Immunolocalization of IL-1â post vanadium exposure.

Immunoreactive cells were induced more in the experimental compared to control as shown in posterior complex and lateral posterior nucleus of thalamus (Fig. **3A** and **3B**), lateral and posterior hypothalamic area (Fig. **3C** and **3D**), motor cortex (Fig. **3E** and **3F**), piriform cortex (Fig. **3G** and **3H**) and entorhinal cortex (Fig. **3I** and **3J**) of experimental mice respectively. Mg .x400

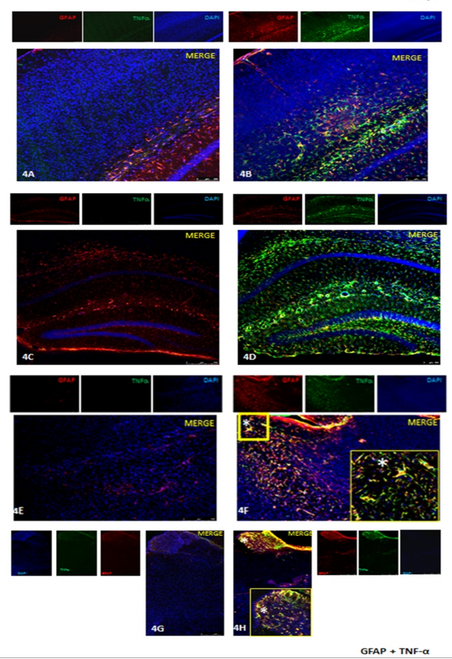

Figure 4: GFAP + TNF-á double labelling

Reactive astrogliosis was seen in the deep cortical and subcortical white matter regions (Fig. **4A** and **4B**), hippocampus (Fig. **4C** and **4D**), internal capsule (Fig. **4E** and **4F**) and habenula nucleus (Fig. **4G** and **4H**). There was a marked induction of TNF-á throughout the deep cortical white matter (Fig. 7B), hippocampus (fig. **4D**), internal capsule (fig. **4 F**) and habenulae nucleus (fig. 7H) regions of experimental compared to controls (Figs. **4A, 4C, 4E** and **4G** respectively). TNF-á induction occurred in astrocytes (colocalization of GFAP + TNF-á).